fibers

MDPI

YAP-Based Fibers Obtained by Internal Crystallization Method

Sergei Mileiko *, Andrew Kolchin, Olga Shakhlevich, Nelly Prokopenko and Sergei Galyshev

Institute of Solid State Physics of Russian Academy of Sciences, 142432 Moscow, Russia
* Correspondence: mileiko@issp.ac.ru

check for updates

Abstract: Two new types of oxide fibers, namely, those of single crystalline yttrium-aluminum perovskite $YAlO_3$ (YAP) and two-phase $YAlO_3$-$Y_4Al_2O_9$ (YAP-YAM), have been grown by the internal crystallization method. The fibers of the second type retain their strength at temperatures up to 1000 °C. Their effective strength in a molybdenum matrix reaches about 600 MPa at a temperature of 1400 °C.

Keywords: oxide fiber; yttrium-aluminum perovskite (YAP); internal crystallization method; microstructure; strength

1. Introduction

Future techniques for energy production call for novel families of heat-resistant materials. Fibrous composites are the most promising as high temperature materials since they incorporate various oxides, carbides, borides, refractive metals and other compounds characterized by high melting points and can be sufficiently creep resistant at high temperatures (see e.g., [1]) and sufficiently tough at ambient temperatures [2]. High and ultra-high temperature materials are of great demand for structural elements subjected to heavy loading and heating in severe environments.

These materials should satisfy numerous requirements. This means that a variety of materials are to be considered as possible candidates for the components of future composites. Oxides are characterized by a number of useful mechanical and physical properties. Therefore, oxide fibers have been developed to be used as reinforcements since the very beginning of the composite era. Sapphire whiskers were the first to be considered as reinforcements for metal matrix composites, but then it became clear that they could not be an effective reinforcement [3]. The invention of a technique of growing sapphire fibers [4] from the melt seemed to provide a new reinforcement for the metal matrix. However, it is well known that sapphire creeps at temperatures higher than 1200 °C and this limits its usage to reinforce metals with relatively low melting temperatures, such as nickel.

A number of techniques have been developed within the last half century to crystallize oxide fibers from the melt, such as Edge Feed Growth (EFG) [4], Laser Heated Pedestal Growth (LHPG) [5], and micro-pulling-down [6]. These techniques allow for the production of fibers of the perfect microstructure necessary for optical and electronic application. However, a low productivity rate of the fabrication processes based on the above techniques makes the fibers too expensive for structural applications.

The internal crystallization method (ICM), invented rather a long time ago [7,8], allows for the crystallization of hundreds and thousands of fibers simultaneously. Hence, the method is a base for developing a fabrication technology of a very high productivity rate, which makes ICM-fibers with a characteristic cross-section size of tens of microns in diameter, suitable for structural applications. A number of single crystalline oxide fibers, including those of mullite [9–11] and yttrium-aluminum garnet [12], which are the most creep-resistant oxides, as well as a number of composite fibers (see e.g., [13–15]), have been obtained and studied since then. However, because the need in

various reinforcements for heat-resistant fibers still remains, the list of oxide fibers studied cannot be considered completed.

In the present paper, the fabrication technique, microstructure and the strength of a new fiber based on yttrium-aluminum perovskite (YAP) are described.

2. Fabrication of the Fibers

The fiber fabrication technology also includes a stage of raw oxide charge preparation. The starting powders for the charge were commercially available Al_2O_3 (the purity is as high as 99.5 wt% and the average size is about 4 microns) and Y_2O_3 (the purity is 99.9% and the size is about 3 microns). Each powder was first heated at a temperature of 900 °C for 5 h for dehydration. Possible agglomerates were then fractured in an agate pounder. The mixture of the powders in the 1:1 molar ratio was then mixed with a solution of polyvinyl butyral in ethanol to form a suspension, which was then homogenized in a high-speed blender. The mixture obtained was dried at a temperature of about 100 °C and then sintered at temperatures 1250–1650 °C. X-ray spectra of the products are presented in Figure 1, and the approximate contents of the phases are given in Table 1.
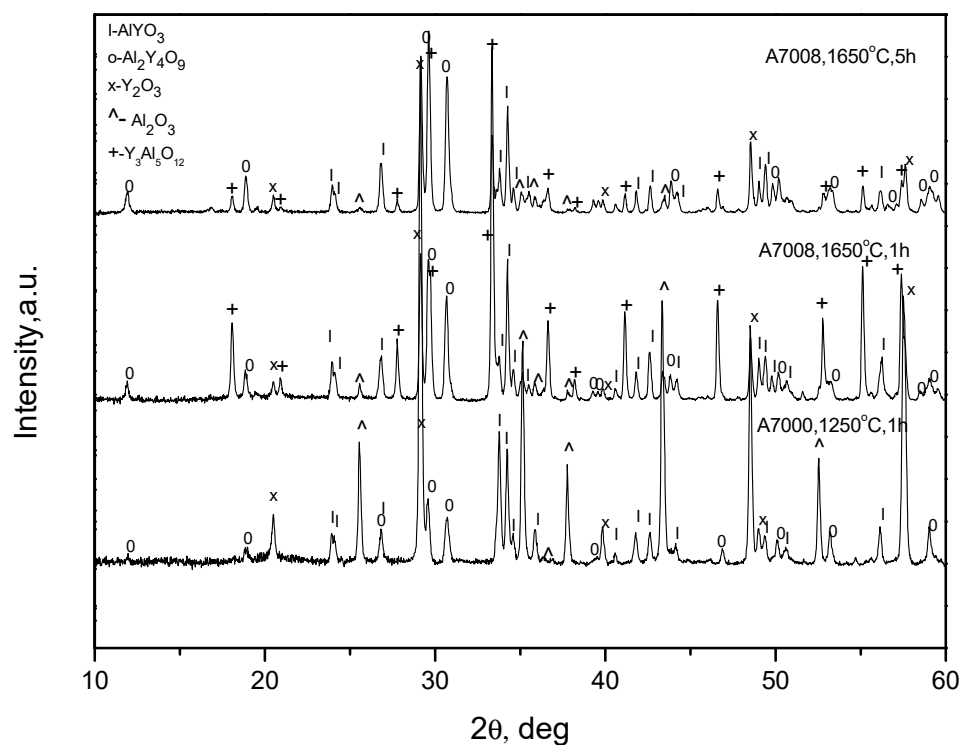

Figure 1. X-ray spectra of the oxide blanks sintered in various temperature/time regimes.

Table 1. Approximate phase compositions of the oxide blanks sintered in various temperature/time regimes.

Sintering Regime		Phase Composition in vol %				
Temperature/°C	Time/h	$YAlO_3$	Al_2O_3	Y_2O_3	$Y_4Al_2O_9$	$Y_3Al_5O_{12}$
1250	1	10	70	15	5	0
1650	1	15	12	10	20	43
1650	5	15	5	15	50	15

It can be seen that no single-phased charges were obtained at any sintering regime. In addition to small contents of $YAlO_3$ (YAP), the $Y_4Al_2O_9$ (YAM) and $Y_3Al_5O_{12}$ (YAG) phases are also present together with the original Al_2O_3 and Y_2O_3 phases. This can possibly be a result of using powders

of rather large sizes, so that the chemical reactions of the YAlO$_3$ synthesis do not go to completion. However, this fact may not be essential since the charges are to be melted.

The fibers were produced by the internal crystallization method (ICM) [7,8]. Two schemes of the fiber crystallization were used. The schematic of the method used in this work is illustrated in Figure 2. A molybdenum carcass with continuous channels in it, which is prepared by diffusion bonding of an assemblage of the wire and foil, is infiltrated with an oxide melt by the capillary force. The melt then crystallizes in the channels to form fibers in an oxide/molybdenum block. Finally, the molybdenum is dissolved in an acid and a bundle of the fibers is ready to be used as a reinforcement. This is a basic scheme, a variation of which was also used in this work.
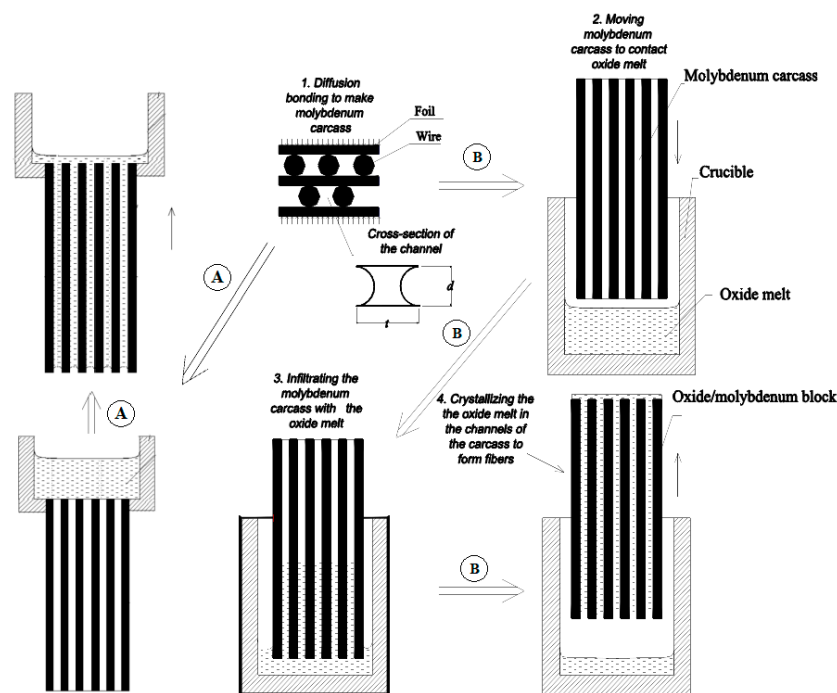

Figure 2. Two schemes of the schematic of the internal crystallization method to produce oxide fibers. The arrows marked by A and B illustrate the sequences of the steps corresponding to the first and second schemes, respectively.

Two schemes of fiber crystallization were used, as shown in Figure 2. In the first scheme, the oxide charge was placed in a molybdenum disposable hopper at the top of the molybdenum carcass. As soon as the melting charge infiltrated the carcass, the oxide/molybdenum block together with the hopper was moved to the cold zone of the furnace. In the second scheme, the charge was placed in a usual molybdenum crucible, as shown in Figure 2, and the melt was kept for 10 min before the molybdenum carcass was immersed into the melt. After the carcass was infiltrated with the oxide melt, it was moved into the cold zone of the furnace. In all experiments, the rate of the oxide/molybdenum block movement was 2 to 250 mm/min. This rate is approximately equal to the crystallization rate of the fibers. The volume fraction of the channels in the molybdenum carcass was 35–40%.

The sizes of the oxide/molybdenum blocks obtained were ~4 × 15 × 65 mm^3. To measure the bending strength of the oxide/molybdenum composites, which gave information about the fiber strength, the block was divided into six specimens of ~4 × 5 × 32 mm^3 in size. Two specimens were tested at room temperature, the other four at high temperatures.

3. Microstructure of the Fibers

Crystallization of the ICM-fibers has some specific features that have been observed in the crystallization of simple oxides like sapphire [7] and complex oxides like mullite [11]. The growth of sapphire fibers starts with a spontaneous crystallization in a certain volume in the vicinity of the oxide/molybdenum block top, which yields a polycrystalline microstructure of the fibers in this volume. The crystals on the solid-liquid boundary then serve as seeds for the rest of the melt in the channels to form single crystal fibers of various crystallographic orientations. In the case of mullite fibers, polycrystalline fibers also grow in the cold volume of oxide/molybdenum block and then the largest crystal grows by absorbing smaller ones to finally occupy the whole cross-section of the channels.

Consider the microstructure of the fibers obtained according to the first scheme. The micrographs presented in Figure 3 show that the microstructure of the fiber is changing along its length. Note that the fibers are composed of two phases. The Y:Al atomic ratio in points 1 and 2 are 1.11 and 2.07, respectively, which means that the "black" phase is $YAlO_3$ and the "grey" one is $Y_4Al_2O_9$.
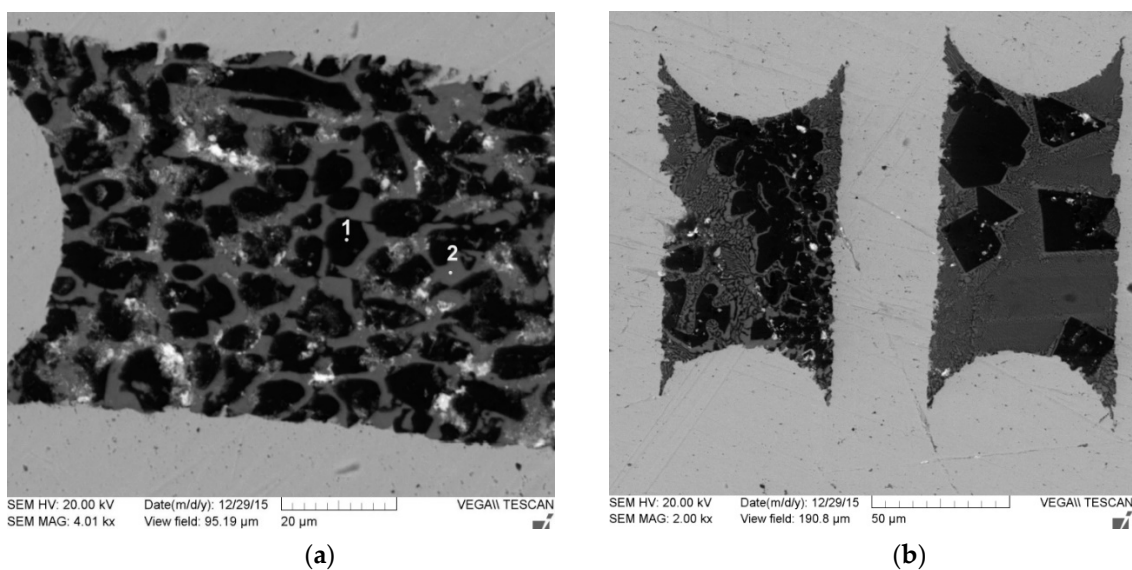

(**a**) (**b**)

Figure 3. SEM micrographs of the fibers at the top (**a**) and bottom (**b**) of an oxide/molybdenum block. The raw material was sintered at 1250 °C and the crystallization rate of the fibers was 10 mm/min. Here and further on, the fiber crystallization starts at the top. The white spots on the micrographs are polishing defects.

The micrographs provide no information on the phase's volume fractions. Inclusions of the second phase ($Y_4Al_2O_9$) are of an elongated shape, as shown in Figure 4a. The cross-sections of the same fibers are presented in Figure 4b. The X-ray spectra of the fibers presented in Figure 5 reveal the presence of $Y_4Al_2O_9$ phase in these fibers. This phase is present in the fibers obtained at all crystallization rates, Figure 6. The temperature/time regimes of the raw charge preparation do not affect the fiber microstructure, see Figures 7 and 8. The measured Y:Al atomic ratios in points 1 and 2 in Figure 7 are 1.09 and 2.16, respectively. Again, it can be seen that the characteristic sizes of the $Y_4Al_2O_9$ phase inclusions are increasing along the fiber length from the top to the bottom.
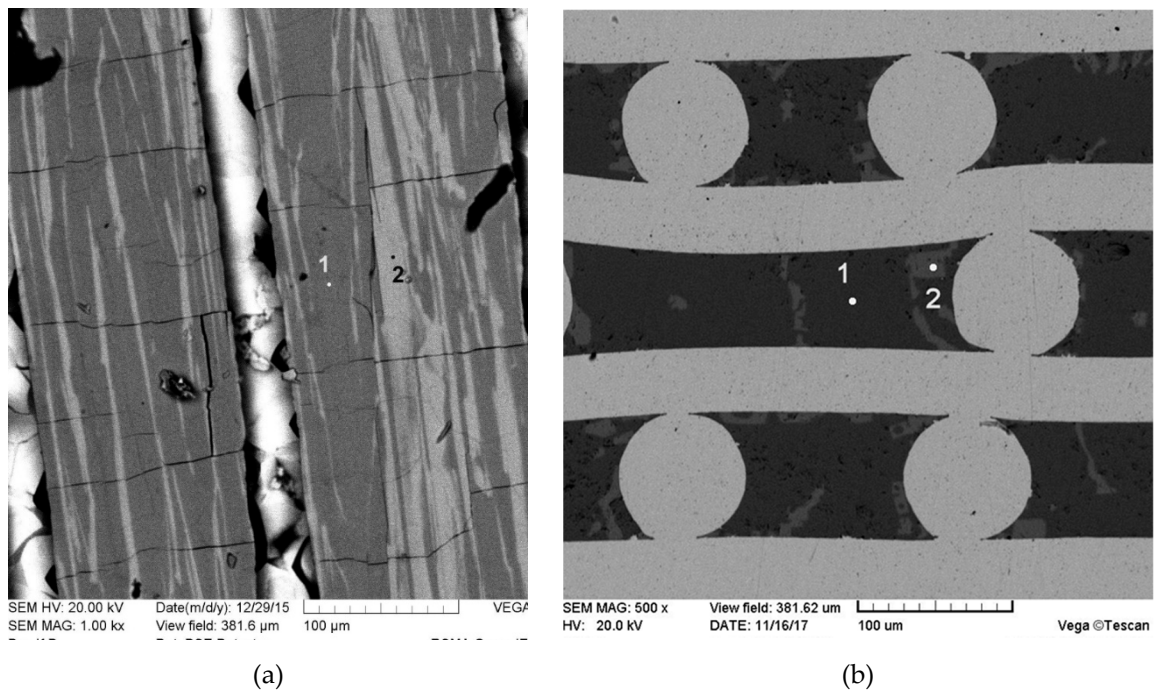
Figure 4. SEM micrographs of the longitudinal (**a**) and transverse (**b**) sections of the composite specimen. The raw material was sintered at 1250 °C and the fiber crystallization rate was 2 mm/min.
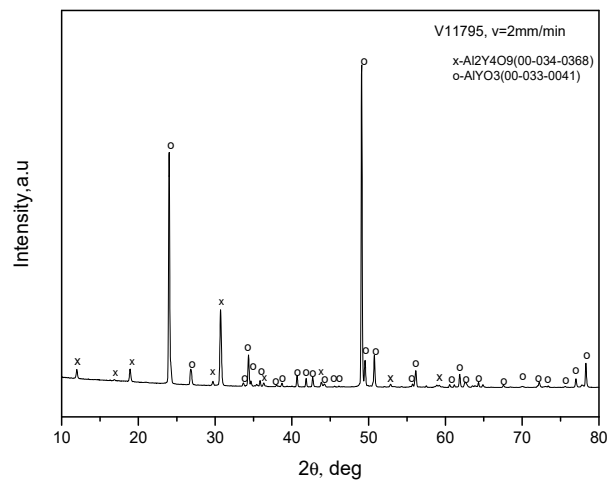

Figure 5. X-ray spectrum of the fibers crystallized at the rate of 2 mm/min. The raw oxide mixture was sintered at 1250 °C. The microstructure of the fibers is presented in Figure 4.
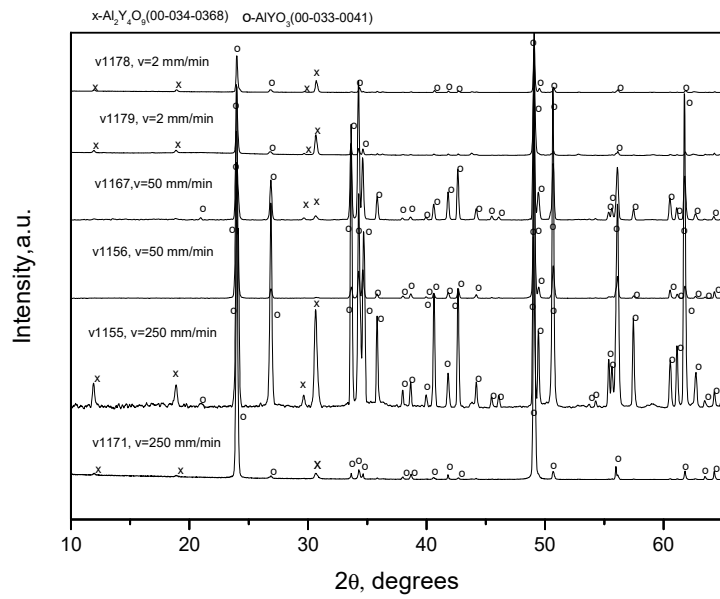
Figure 6. X-ray spectra of the fibers crystallized at various rates. The raw oxide mixture was sintered at 1250 °C.

Figure 7. *Cont.*

Top   Bottom
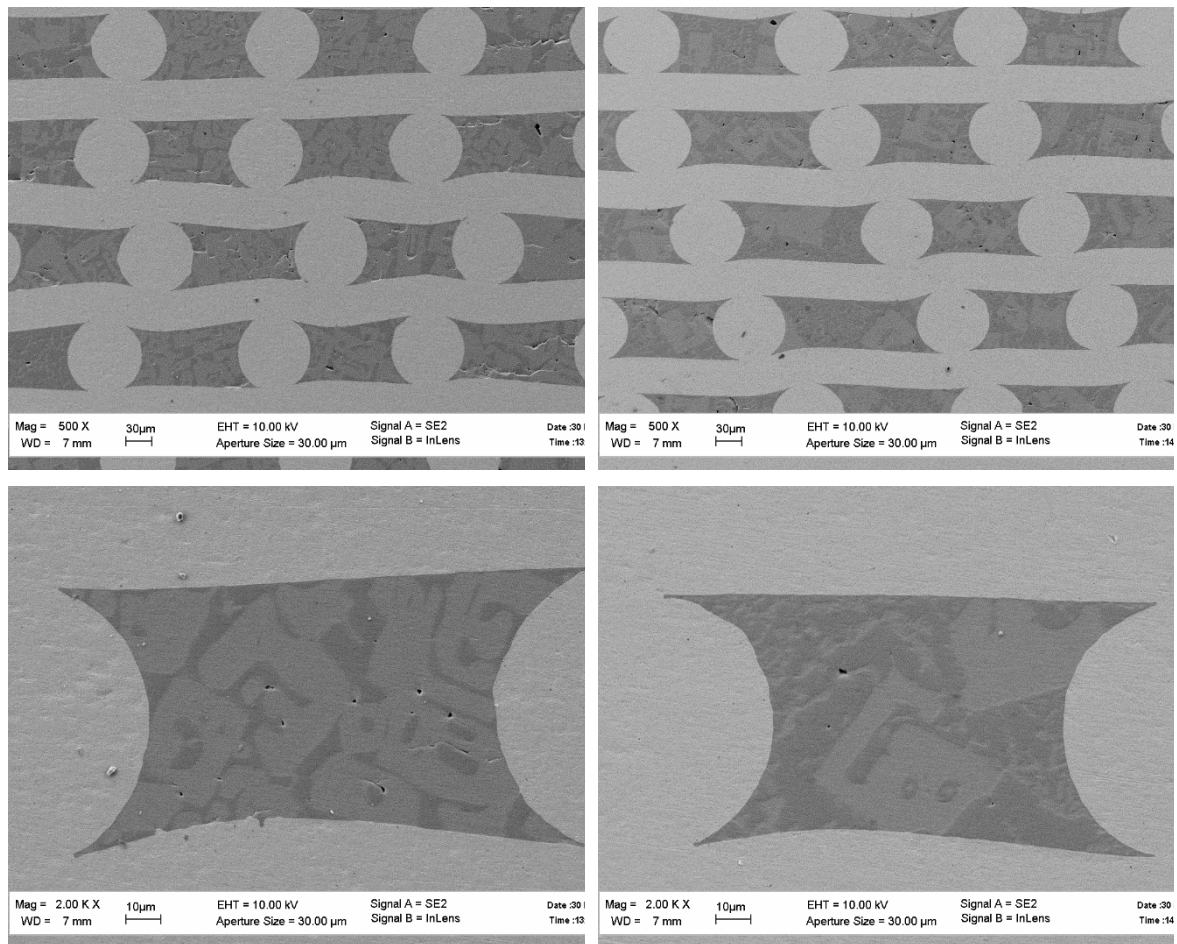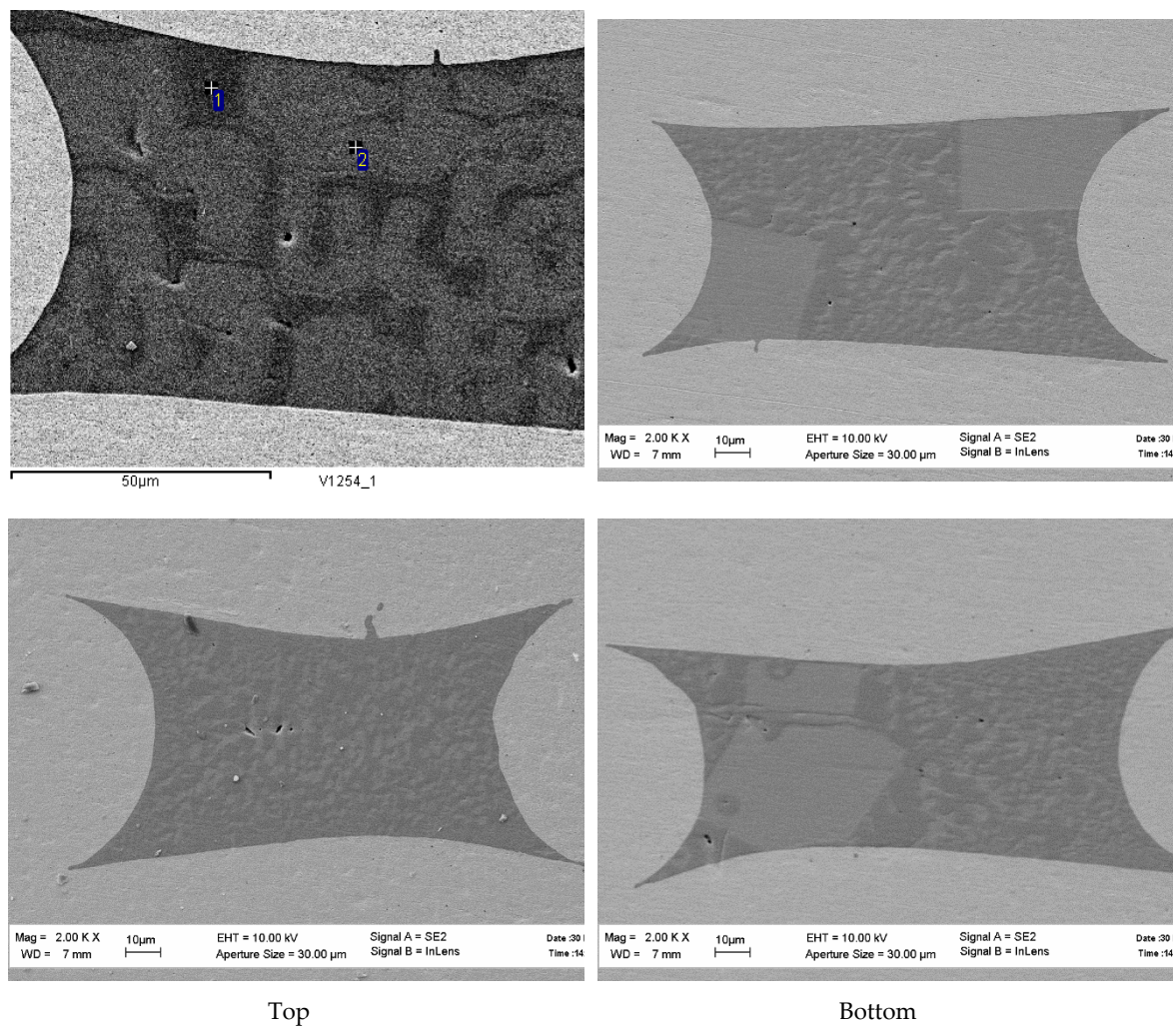
Figure 7. SEM micrographs of the cross-sections of the composite specimen V1254 crystallized at a rate of 50 mm/min according to the first crystallization scheme from the raw oxide mixture sintered at 1650 °C for 5 h. Note a difference between the fiber microstructures at top and bottom of the oxide/molybdenum block.
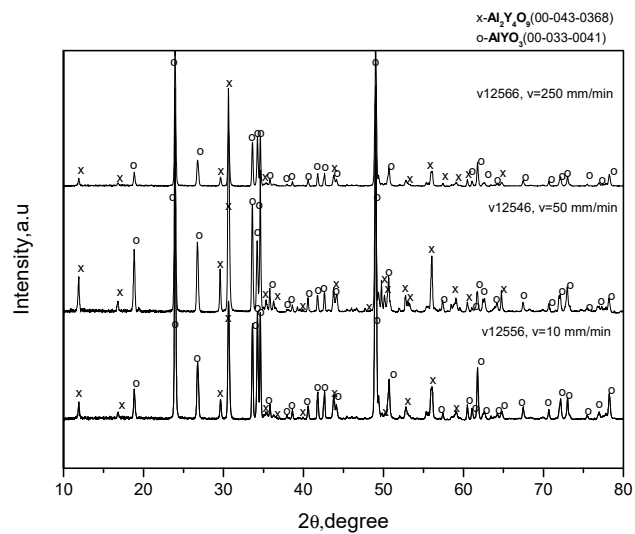

Figure 8. X-ray spectra of the fibers crystallized from the raw oxides sintered at 1650 °C at the crystallization rates shown in the graph fields.

It should be noted that the microstructures of composite fibers obtained by using the first crystallization scheme vary from specimen to specimen. These observations pose two questions.

First, why the $Y_4Al_2O_9$ phase occurs in the fibers despite the original composition of the raw oxide mixture corresponding to $YAlO_3$. Second, why the description of these fibers was included in this paper.

The answer to the first question can be found in Table 1, which presents the composition of the charge to be melted in the hopper located at the top of the molybdenum carcass. It can be seen that the charge contains a variety of phases including $Y_4Al_2O_9$, $Y_3Al_5O_{12}$ and the original yttria and alumina phases. Note that the oxide/molybdenum block starts to be moved to the cold zone of the furnace as soon as the channels in the carcass are filled with the oxides that can be seen on the bottom of the block. Presumably, heating the charge above 1650 °C leads to an additional synthesis of $YAlO_3$ and $Y_4Al_2O_3$ and both phases infiltrate the channels in the carcass leaving a scrap in the hopper. The absence of the yttrium-aluminum garnet $Y_3Al_5O_{12}$ in the fibers can, probably, be explained by the specific features of the crystallization of this garnet from the melt [16].

The answer to the second question will be given below when discussing the fiber strength.

The infiltration process cannot be controlled and this can explain a variety of the fiber microstructures obtained. This can result in a scatter of the fiber strength.

Crystallizing the fibers according to the second scheme, by melting the charge in the crucible and keeping the melt in the crucible for some time before the carcass moves into the melt, yields single-phased $YAlO_3$ fibers. Indeed, the X-ray spectra of the melt after keeping it for 20 min in the crucible, Figure 9, contain peaks corresponding to $YAlO_3$ and some small peaks that cannot be ascribed to any known compounds that can be a result of chemical interactions between the oxide melt and molybdenum.
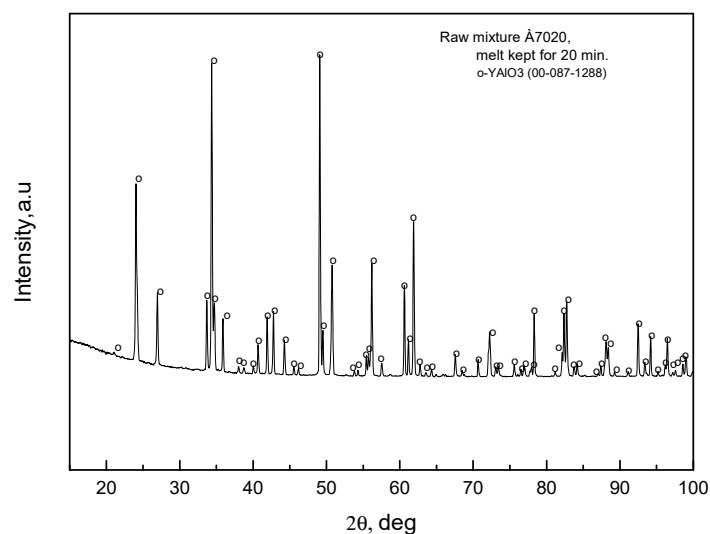

Figure 9. X-ray spectrum of raw oxides kept melted for 20 min.

The crystal structure of the YAP fibers was studied by the X-ray Xcaliber Gemini R diffractometer (graphite monochromator, MoK_λ radiation, two-coordinates CCD imager). It was found that all fibers are single crystalline with the orthorhombic lattice Pnma, a = 5.215, b = 5.341, c = 7.387. The fibers have a sufficiently homogeneous microstructure, presented in Figure 10.
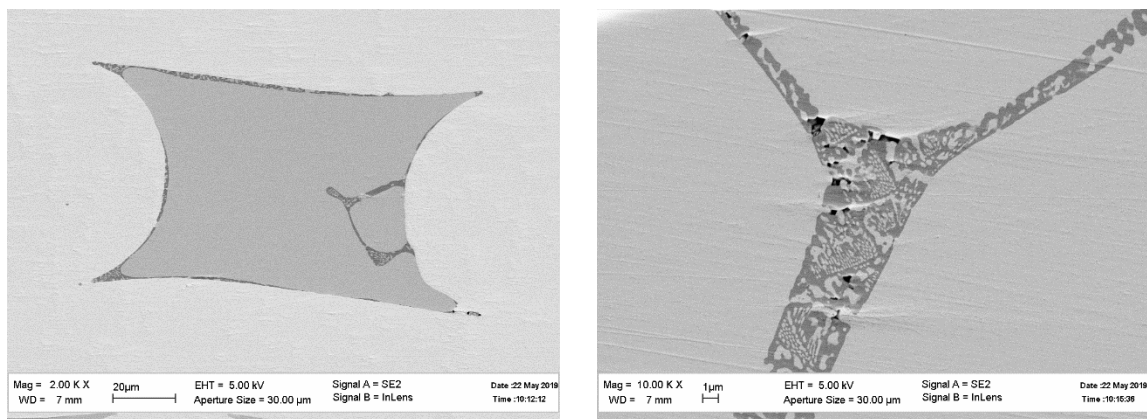
Figure 10. SEM micrographs of the cross-section of the fibers obtained according to the second crystallization scheme.

4. Strength of the Fibers

The room temperature fiber strength was measured by testing oxide/molybdenum composites in a three-point bending test using a universal testing machine with a computer recording the load/displacement curve. High temperature testing was done in a vacuum. Only the load/time curves were recorded since the testing machine did not have an extensometer.

Actually, this procedure gave the effective strength of the fiber in the matrix [17]. To calculate the fiber strength according to the rule of mixture, the values of the strength of the recrystallized molybdenum were assumed to be 450, 109, 85, 78 and 62 MPa at temperatures 20 °C, 1000 °C, 1200 °C, 1300 °C and 1400 °C, respectively [18]. The fiber volume fraction was taken as 0.37.

The dependence of fiber strength on the crystallization rate is presented in Figure 11. It can be seen that:

- There is a large scatter in the strengths of the composite fibers obtained according to the first scheme of crystallization that are composed of two phases, YAP and YAM. This can be a result of the variability of the microstructure of such fibers;
- The strength scatter of the fibers obtained according to the second scheme, which contain only single crystalline YAP, seems to be much smaller;
- The mean strength values of the two types of fibers are nearly the same for crystallization rates from 2 to 50 mm/min. But some composite fibers (the second crystallization scheme) have very high strength values (>1000 MPa);
- Crystallizing fibers at the rate of 250 mm/min provides an interesting result: the mean strength of the composite fibers is essentially higher than that of pure $YAlO_3$ fibers. Perhaps this resembles the behavior of a composite system close to the composition of the eutectic one. Hence, the idea to study the mechanical behavior of the YAP-YAM system more accurately looks attractive. The idea is to be realized in a coming work.

The strength/temperature dependence of the YAP-YAM-fiber/molybdenum-matrix composites is presented in Figure 12. The composite strength at temperatures 1000–1400 °C does not depend on the crystallization rate. Hence, the temperature dependence of the fiber strength is presented in Figure 13 without indicating the crystallization rate. It can be seen that the YAP-YAM fibers retain their strength to a temperature of 1000 °C. Then their strength slightly decreases. The strength value at 1400 °C is still sufficiently high, being 539 ± 80 MPa.
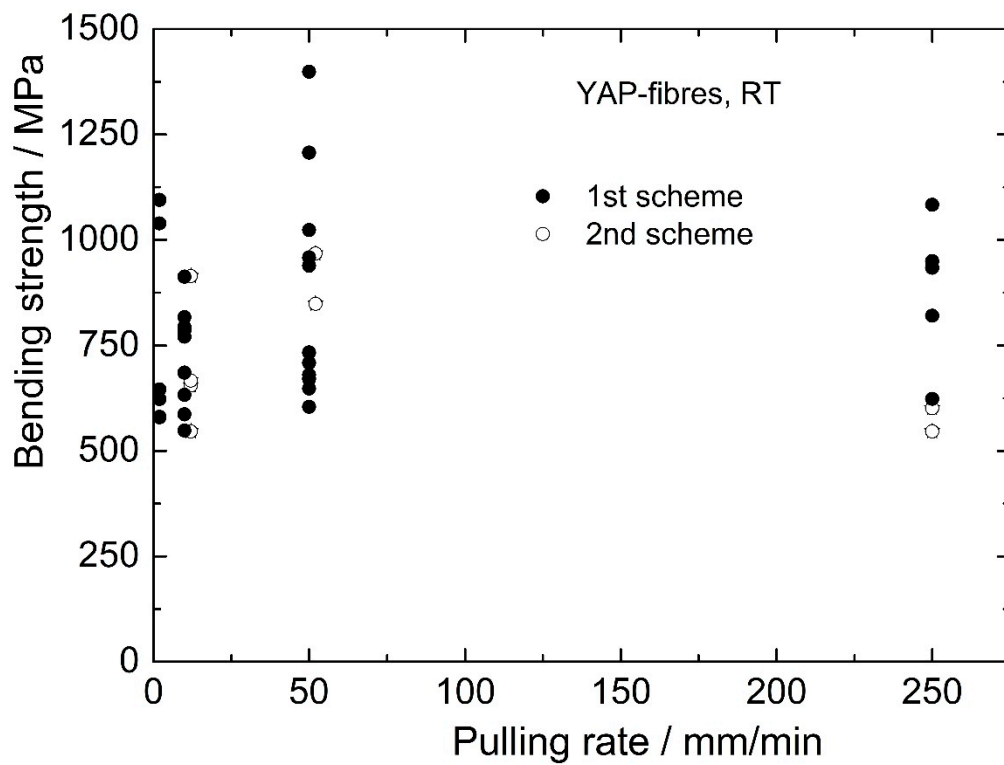
Figure 11. Dependence of the effective strength of the fibers on the crystallization rate.
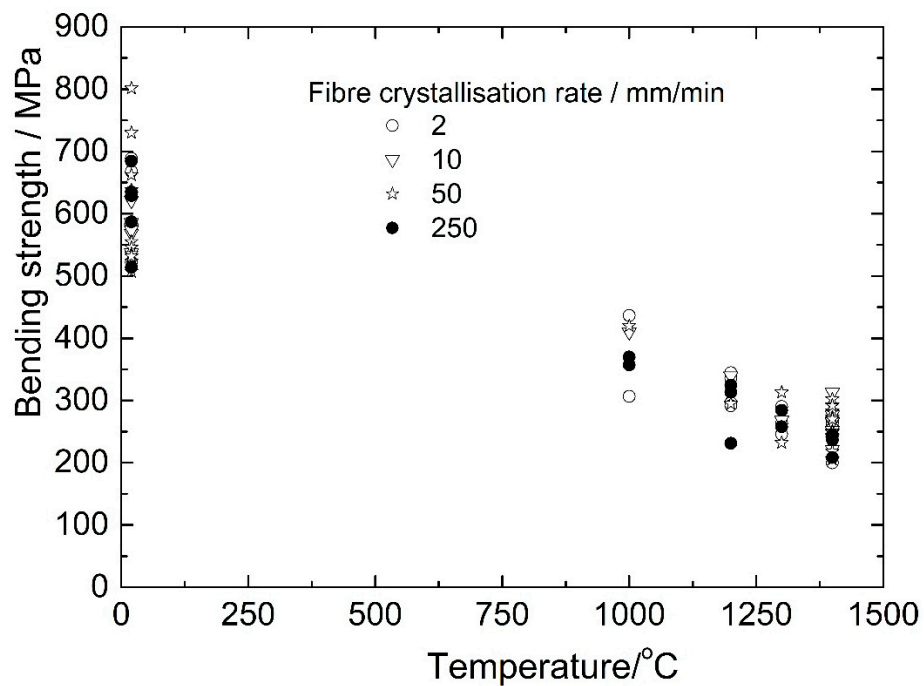

Figure 12. Strength/temperature dependence of the oxide/molybdenum composites produced according to the first scheme of fiber crystallization.
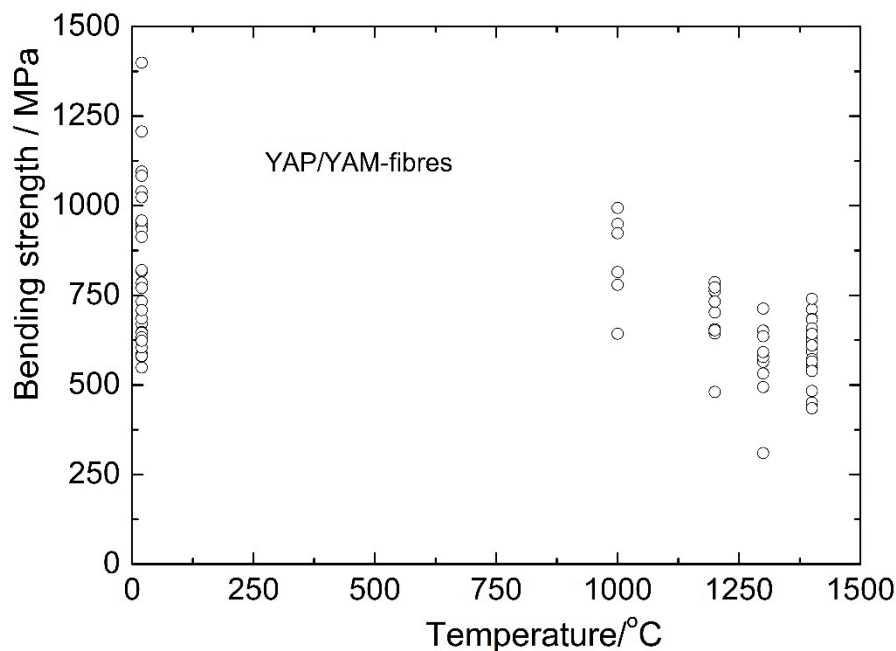
Figure 13. Strength/temperature dependence of the two-phase fibers.

5. Conclusions

1. Single crystalline fibers of yttrium-aluminum perovskite $YAlO_3$ (YAP) and two-phase $YAlO_3$-$Y_4Al_2O_9$ (YAP-YAM) composite fibers have been obtained for the first time.
2. Both types of fibers are sufficiently strong.
3. Composite fibers retain their strength to a temperature of about 1000 °C. The mean strength value at 1400 °C is close to 600 °C.
4. Two-phase YAP-YAM composite fibers challenge more thoroughly studies focusing, in particular, on the fibers of the eutectic composition.

Author Contributions: Conceptualization, S.M.; methodology, S.M. and A.K.; investigation, O.S., N.P. and S.G.; writing—original draft preparation, N.P.; writing—review and editing, S.M.; project administration, S.M.

References

1. Mileiko, S.T. High temperature molybdenum matrix composites. *Ceram. Int.* **2019**, *45*, 9439–9443. [CrossRef]
2. Mileiko, S.T. Fracture-toughness/notch-sensitivity correlation for metal- and ceramic-based fibrous composites. *Compos. Part B* **2017**, *116*, 1–6. [CrossRef]
3. Calow, C.A.; Moore, A. No hope for ceramic whiskers or fibers as reinforcement of metal matrix at high temperatures. *J. Mater. Sci.* **1972**, *7*, 543–558. [CrossRef]
4. LaBelle, H.E., Jr.; Mlavsky, A.I. Growth of sapphire filaments from the melt. *Nature* **1967**, *216*, 574–575. [CrossRef]
5. Feigelson, R.S. Pulling optical fibers. *J. Cryst. Growth* **1986**, *79*, 669–680. [CrossRef]
6. Fukuda, T. Basics of the μ-PD method. In *Shaped Crystals: Growth by Micro-Pulling-Down Technique*; Springer: Berlin, Germany, 2007; pp. 27–45.

7.   Mileiko, S.T.; Kazmin, V.I. Crystallization of fibers inside a matrix: A new way of fabrication of composites. *J. Mater. Sci.* **1992**, *27*, 2165–2172. [CrossRef]

8.   Mileiko, S.T.; Kazmin, V.I. Structure and mechanical properties of oxide fiber reinforced metal matrix composites produced by the internal crystallization method. *Compos. Sci. Technol.* **1992**, *45*, 209–220. [CrossRef]

9.   Mileiko, S.T.; Kiiko, V.M.; Starostin, M.Y.; Kolchin, A.A.; Kozhevnikov, L.S. Fabrication and some properties of single crystalline mullite fibers. *Scr. Mater.* **2001**, *44*, 249–255. [CrossRef]

10.   Rüscher, C.H.; Mileiko, S.T.; Schneider, H. Mullite single cyrystal fibers produced by the Internal Crystallization Method (ICM). *J. Eur. Ceram. Soc.* **2003**, *23*, 3113–3117. [CrossRef]

11.   Mileiko, S.T.; Serebryakov, A.V.; Kiiko, V.M.; Kolchin, A.A.; Kurlov, V.N.; Novokhatskaya, N.I. Single crystalline mullite fibers obtained by the internal crystallization method: Microstructure and creep resistance. *J. Eur. Ceram. Soc.* **2009**, *29*, 337–345. [CrossRef]

12.   Mileiko, S.T.; Kurlov, V.N.; Kolchin, A.A.; Kiiko, V.M. Fabrication, properties and usage of single-crystalline YAG fibers. *J. Eur. Ceram. Soc.* **2002**, *22*, 1831–1837. [CrossRef]

13.   Mileiko, S.T.; Kiiko, V.M.; Sarkissyan, N.S.; Starostin, M.Y.; Gvozdeva, S.I.; Kolchin, A.A.; Strukova, G.K. Microstructure and properties of Al_2O_3-$Al_5Y_3O_{12}$ fiber produced via internal crystallization route. *Compos. Sci. Technol.* **1999**, *59*, 1763–1772. [CrossRef]

14.   Mileiko, S.T.; Kolchin, A.A.; Novokhatskaya, N.I.; Prokopenko, N.A.; Shakhlevich, O.F. Mullite-zirconia fibers produced by internal crystallization method: Microstructure and strength properties. *Compos. Part A* **2018**, *112*, 405–414. [CrossRef]

15.   Mileiko, S.; Kolchin, A.; Kiiko, V.; Novokhatskaya, N. Composite oxide fibers grown by internal crystallization method. *Fibers* **2017**, *5*, 48. [CrossRef]

16.   Bondar, I.A.; Koroleva, L.N.; Bezruk, E.T. Physical-chemical properties of yttrium gallates and aluminates. *Inorg. Mater.* **1984**, *20*, 257–267. (In Russian)

17.   Mileiko, S.T.; Sarkissyan, N.S.; Kolchin, A.A.; Kiiko, V.M. Oxide fibers in a Ni-based matrix—Do they degrade or become stronger? *J. Mater. Des. Appl.* **2004**, *218*, 193–200.

18.   Mileiko, S.T. *Metal and Ceramic Based Composites*; Elsevier: Amsterdam, The Netherlands, 1997; p. 598.